Acoustic scattering from a submerged cylindrical shell coated with locally resonant acoustic metamaterials*

Li Li(李 黎), Wen Ji-Hong(温激鸿), Cai Li(蔡 力), Zhao Hong-Gang(赵宏刚), and Wen Xi-Sen(温熙森)†

Key Laboratory of Photonic and Phononic Crystal of Ministry of Education, National University of Defense Technology, Changsha 410073, *China*
Laboratory of Science and Technology on Integrated Logistics Support, National University of Defense Technology, Changsha 410073, *China*

(Received 29 March 2012; revised manuscript received 18 June 2012)

Using the multilayered cylinder model, we study acoustic scattering from a submerged cylindrical shell coated with locally resonant acoustic metamaterials, which exhibit locally negative effective mass densities. A spring model is introduced to replace the traditional transfer matrix, which may be singular in the negative mass region. The backscattering form function and the scattering cross section are calculated to discuss the acoustic properties of the coated submerged cylindrical shell.

Keywords: acoustic metamaterials, acoustic scattering, cylindrical shell

PACS: 43.20.+g, 42.25.Bs, 52.35.Dm **DOI:** 10.1088/1674-1056/22/1/014301

1. Introduction

Recently, acoustic metamaterials,[1,2] analogous to their electromagnetic counterparts, have received growing attention from the scientific community. The acoustic metamaterials, which exhibit negative effective parameters, offer new insights into acoustic wave propagation. Attention has mainly focused on the design and experimental demonstration[3–9] of the acoustic metamaterials, and their applications for ultrasonic focusing and imaging,[10,11] acoustic cloak,[12–14] and so on. In 2006, Zhao *et al*.[15–17] showed that the locally resonant acoustic metamaterial slab composed of silicon rubber-coated lead spheres embedded in an epoxy host is effective for sound absorbing in the resonant frequency region with the viscosity of the component being considered. Yet to the best of our knowledge, evaluating the effect of the acoustic metamaterials coated on the cylindrical shells remains unexplored, which constitutes an important underwater acoustic problem. With this purpose, we propose in this paper a general model on acoustic scattering from a submerged cylindrical shell coated with acoustic metamaterials.

The paper is organized as follows. In Section 2, we propose the model for a submerged cylindrical shell coated with locally resonant acoustic metamaterials, showing how the acoustic scattering of the shell is calculated using the multilayered cylinder model. In Section 3, a numerical example is presented to demonstrate the acoustic properties of the cylindrical shell coated with the locally resonant acoustic metamaterials exhibiting negative mass density. Finally, the paper is summarized in Section 4.

2. Model and method

Figures 1(a) and 1(b) show a cylindrical shell coated with locally resonant acoustic metamaterials and immersed in an infinite ideal fluid (water). The shell is made of steel, with r_1 and r_2 representing its inner and outer radii, respectively. The coating is composed of coated solid spheres embedded in a solid host, with r_3 representing its outer radius and ϕ the fill fraction. For the components of the coating, r_s and r_c denote the radii of the uncoated and the coated solid spheres, respectively, as shown in Fig. 1(c). The cylindrical shell is of infinite length in the z direction and air-filled. Assume a time-harmonic, plane longitudinal wave incident normally on the shell along the x direction, as shown in Fig. 1(b).

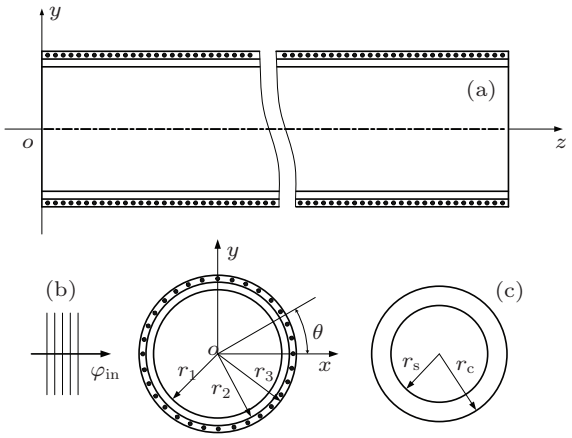


Fig. 1. (a) Schematic diagram of a cylindrical shell coated with locally resonant acoustic metamaterials. (b) Cross-sectional view (right) of the coated cylindrical shell. (c) Schematic diagram of a coated sphere. The φ_{in} indicates a time-harmonic, plane longitudinal acoustic wave incident normally along the x direction.

*Project supported by the National Natural Science Foundation of China (Grant Nos. 11004249 and 11004250).
†Corresponding author. E-mail: wenxs@vip.sina.com
© 2013 Chinese Physical Society and IOP Publishing Ltd

Although the elastic wave propagation in a three-dimensional periodic structure is not isotropic, recent work showed that the anisotropy effect can be neglected for low filling fractions.[18] Thus the locally resonant acoustic metamaterial coating can be regarded as an isotropic homogeneous layer with effective material parameters. An isotropic elastic material is known to be completely described through its mass density ρ, bulk modulus κ, and shear modulus μ, which are constants in common conception. However, the dynamic effective material parameters, indicated by ρ_{eff}, κ_{eff}, and μ_{eff}, are frequency dependent in the frequency domain, which describe the dynamic behavior of the coating in macroscopic detail. Zhou *et al.* presented an analytic model for the effective parameters of the locally resonant acoustic metamaterials within the long-wavelength limit as[19]

$$\begin{aligned}
\rho_{\text{eff}} &= \rho_{\text{h}} \frac{\phi_{\text{s}} \langle \boldsymbol{p} \rangle_{\text{s}} + \phi_{\text{c}} \langle \boldsymbol{p} \rangle_{\text{c}} + \phi_{\text{h}} \langle \boldsymbol{p} \rangle_{\text{h}}}{\langle \boldsymbol{p} \rangle_{\text{h}}}, \\
\kappa_{\text{eff}} &= \frac{\kappa_{\text{s}} \phi_{\text{s}} \langle \varepsilon_{\text{b}} \rangle_{\text{s}} + \kappa_{\text{c}} \phi_{\text{c}} \langle \varepsilon_{\text{b}} \rangle_{\text{c}} + \kappa_{\text{h}} \phi_{\text{h}} \langle \varepsilon_{\text{b}} \rangle_{\text{h}}}{\phi_{\text{s}} \langle \varepsilon_{\text{b}} \rangle_{\text{s}} + \phi_{\text{c}} \langle \varepsilon_{\text{b}} \rangle_{\text{c}} + \phi_{\text{h}} \langle \varepsilon_{\text{b}} \rangle_{\text{h}}}, \\
\mu_{\text{eff}} &= \frac{\mu_{\text{s}} \phi_{\text{s}} \langle e \rangle_{\text{s}} + \mu_{\text{c}} \phi_{\text{c}} \langle e \rangle_{\text{c}} + \mu_{\text{h}} \phi_{\text{h}} \langle e \rangle_{\text{h}}}{\phi_{\text{s}} \langle e \rangle_{\text{s}} + \phi_{\text{c}} \langle e \rangle_{\text{c}} + \phi_{\text{h}} \langle e \rangle_{\text{h}}},
\end{aligned} \tag{1}$$

where $\langle \boldsymbol{p} \rangle$, $\langle \varepsilon_{\text{b}} \rangle$, $\langle e \rangle$, ρ, κ, and μ represent the momentum, bulk strain, averaging shear strain, density, bulk modulus, and shear modulus of the component of the locally resonant acoustic metamaterials, respectively, and subscripts s, c, and h indicate the sphere, the coating, and the host material, respectively. Fill fractions of the components are defined by $\phi_{\text{s}} = (r_{\text{s}}/r_{\text{h}})^3$, $\phi_{\text{c}} = \phi - \phi_{\text{s}}$, $\phi_{\text{h}} = 1 - \phi$, and r_{h} is defined as $r_{\text{h}} = r_{\text{c}}/\sqrt[3]{\phi}$.

The analytic model can reveal clearly the physical mechanism of the negative effective parameters induced by the resonant effect. By taking the locally resonant acoustic metamaterials of rubber-coated lead spheres in an epoxy as a prototype, it is found that the negative effective mass density may arise from the negative total momentum of the unit cell with positive velocity fields due to the local resonance.[19,20]

Let us consider the acoustic scattering from the coated shell by using the multilayered cylinder model.[21,22] As the cylindrical shell is of infinite length in the z direction, the scalar potentials for incident and scattered longitudinal waves in the surrounding fluid can be expanded in cylindrical Bessel and Hankel functions respectively as

$$\begin{aligned}
\varphi_{\text{in}} &= \mathrm{e}^{\mathrm{i}k_{\text{w}}x} = \sum_{n=-\infty}^{\infty} (\mathrm{i})^n \mathrm{J}_n(k_{\text{w}}r)\, \mathrm{e}^{\mathrm{i}n\theta}, \\
\varphi_{\text{s}} &= \sum_{n=-\infty}^{\infty} A_n \mathrm{H}_n(k_{\text{w}}r)\, \mathrm{e}^{\mathrm{i}n\theta},
\end{aligned} \tag{2}$$

where $\mathrm{J}_n(\cdot)$ and $\mathrm{H}_n(\cdot)$ are the n-th order cylindrical Bessel and Hankel functions of the first kind, respectively, and k_{w} represents the longitudinal wave number in water. The time factor $\mathrm{e}^{-\mathrm{i}\omega t}$ in φ_{in} and φ_{s} is dropped throughout.

Generally, for a multilayered cylinder, the stresses and displacements on the outer and inner boundaries of the j-th layer can be related by a transfer matrix $\boldsymbol{T}_n^j$, which is in terms of cylindrical Bessel and Neumann functions. The total transfer matrix $\boldsymbol{T}_n$, which relates the stresses and displacements in the surrounding water and in the inner core of air, is obtained by the products of $\boldsymbol{T}_n^j$. Combining Eq. (2) and $\boldsymbol{T}_n$, we obtain a linear system of equations for the multilayered cylinder, which gives the scattering coefficients A_n. Once the scattering coefficients are obtained, the far-field backscattering form function $f_\infty(\theta = \pi)$ and the total scattering cross section Q_{l} can be found as

$$\begin{aligned}
f_\infty(\theta = \pi) &= \frac{2\sqrt{2}}{\sqrt{\pi k_{\text{w}} r_3}} \left| \sum_{n=-\infty}^{\infty} \mathrm{i}^n A_n \right|, \\
Q_{\text{l}} &= \frac{1}{k_{\text{w}} r_3} \sum_{n=-\infty}^{\infty} |A_n|^2.
\end{aligned} \tag{3}$$

Although the multilayered cylinder model has been demonstrated to be effective for general elastic materials,[21] our study has shown that the results may present a strong singularity when the layer exhibits negative material parameters. As is mentioned above, the transfer matrix $\boldsymbol{T}_n^j$, which relates the stresses and displacements on the outer and inner boundaries of the j-th layer, is in terms of cylindrical Bessel and Neumann functions. When kr is real, the Bessel function is known to oscillate in a limited range. However, when kr is imaginary, corresponding to the negative effective material parameters, the Bessel function of complex variables may exhibit divergence.[23] Similar phenomena can be found in the Hankel and Neumann functions. Thus the transfer matrix $\boldsymbol{T}_n^j$ may be singular in the negative parameter frequency range.

To resolve this problem, a spring model for the thin cylindrical layer is introduced to replace the transfer matrix $\boldsymbol{T}_n^j$. The transfer matrix $\boldsymbol{T}_n^j$ is firstly expanded in series and simplified as the first-order asymptotic transfer matrix by truncating the high-order components. When the layer is thin, i.e., the thickness h is far less than the radius, we can further simplify the transfer matrix $\boldsymbol{T}_n^j$ as[24]

$$\boldsymbol{T}_n^{j*} = \begin{bmatrix} 1 & 0 & \dfrac{h}{\lambda + 2\mu} & 0 \\ 0 & 1 & 0 & \dfrac{h}{\mu} \\ -\rho h \omega^2 & 0 & 1 & 0 \\ 0 & -\rho h \omega^2 & 0 & 1 \end{bmatrix}, \tag{4}$$

where $h = r_j - r_{j-1}$ indicates the thickness of the layer, and ρ and λ, μ indicate the density and the Lamé's constants, respectively.

According to Eq. (4), the stresses and displacements on the outer and inner boundaries of the j-th layer can be described by

$$\begin{cases} \sigma_{rr}(r_{j-1}) = K_{\text{N}} \left[u_r(r_j) - u_r(r_{j-1}) \right], \\ \sigma_{r\theta}(r_{j-1}) = K_{\text{T}} \left[u_\theta(r_j) - u_\theta(r_{j-1}) \right], \end{cases} \tag{5}$$

$$\begin{cases} \sigma_{rr}(r_j) - \sigma_{rr}(r_{j-1}) = -\omega^2 m u_r(r_{j-1}), \\ \sigma_{r\theta}(r_j) - \sigma_{r\theta}(r_{j-1}) = -\omega^2 m u_\theta(r_{j-1}). \end{cases} \quad (6)$$

Thus the layer can be described physically by a two-dimensional mass–spring model, with $K_N = (\lambda + 2\mu)/h$ and $K_T = \mu/h$ representing the stiffnesses of the longitudinal and the transverse springs, respectively, and $m = \rho h$ the mass.

In this case, the Bessel function serials are not involved in Eq. (4), thus the problem of singularity can be avoided.

3. Results and discussion

In order to verify our theory, the scattering wave field of the coated shell shown in Fig. 1 in a square area of 10 m×10 m is calculated by both the above theory and the COMSOL Multiphysics. Figure 2 shows the scattering wave fields calculated by these two methods. Material parameters of the coating are set as $\rho_{\text{coating}} = -1208$ kg/m^3, $E_{\text{coating}} = 7.67 \times 10^8$ Pa, and $\sigma_{\text{coating}} = 0.28$. Geometry parameters are $r_1 = 2.975$ m, $r_2 = 3.025$ m, and $r_3 = 3.075$ m. The frequency is $f = 630.39$ Hz. Boundary conditions on the four edges of the square area are set to be radiation conditions to simulate the infinite out surrounding water on COMSOL. A good agreement between the two results can be observed, which means that the spring model is valid to describe the elastic wave propagation in the thin metamaterial layer with a negative mass.

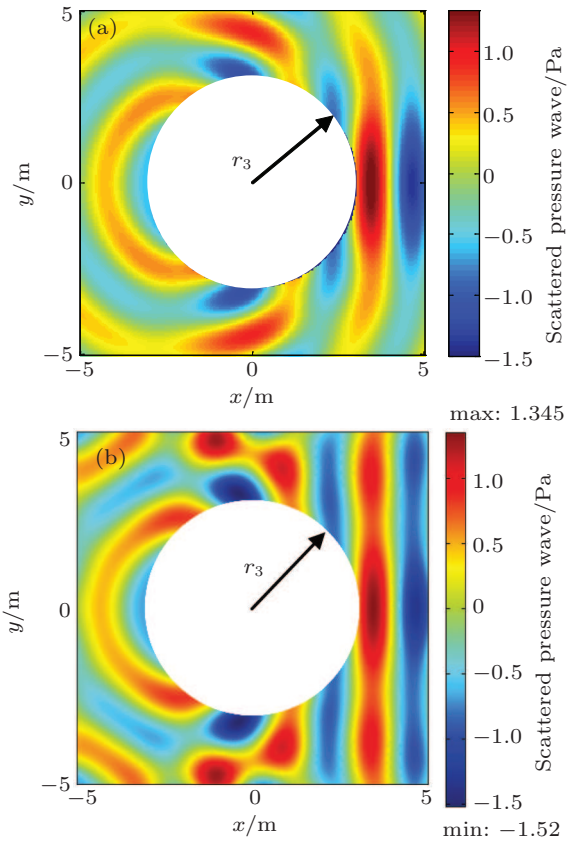


Fig. 2. (color online) The scattering wave fields in the surrounding water in the near-field calculated by (a) our method and (b) on COMSOL.

As a numerical example, we investigate the far-field backscattering form function $f_\infty(\theta = \pi)$ and the total scattering cross section Q_l of a submerged cylindrical shell coated with locally resonant acoustic metamaterials, which are defined in Eq. (3). The coating is composed of silicon rubber-coated steel spheres embedded in a rubber host. The geometry parameters, shown in Fig. 1, are given as $r_1 = 4.975$ m, $r_2 = 5.025$ m, $r_3 = 5.041$ m, $r_s = 0.005$ m, and $r_c = 0.007$ m. Material parameters employed are listed in Table 1.

Table 1. Parameters of the materials employed in this study.

Material	ρ/kg·m^{-3}	c_l/m·s^{-1}	c_t/m·s^{-1}
Steel	7670	6010	3231
Silicon rubber	1300	23	6
Rubber	1100	920	90
Water	1000	1500	
Air	1.29	340	

Figure 3 shows the effective material parameters of the locally resonant acoustic metamaterials. We can see in the figure that the effective mass density is frequency dependent in the frequency domain. The shadow region shown in Fig. 3 corresponding to the first negative-mass band takes place in a frequency range from 522 Hz to 753 Hz, which is induced by the negative momentums of the steel sphere with respect to the rubber host. In contrast, the effective bulk and shear moduli are both positive in the whole frequency range, thus we consider the coating belongs to the single negative metamaterials.

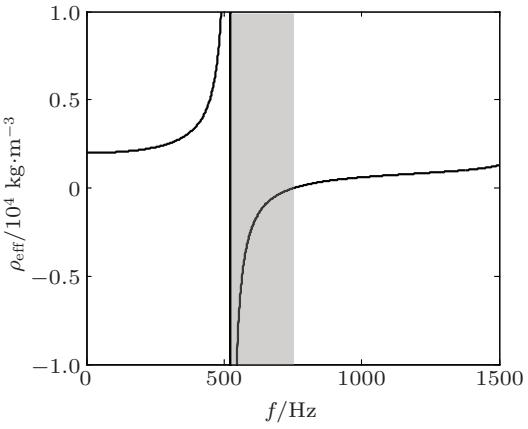


Fig. 3. The effective mass density ρ_{eff} of the locally resonant acoustic metamaterial coating.

Figure 4 shows the far-field backscattering form function and the total scattering cross section for the coated shell shown in Fig. 1. In each panel, the scattering form function and the scattering cross section are each given as a function of frequency with the viscosity of the coating considered. The viscosity is denoted by complex effective Lamé's constants, i.e., $\lambda = \lambda_{\text{eff}}(1 - i\eta)$ and $\mu = \mu_{\text{eff}}(1 - i\eta)$, where λ_{eff}, μ_{eff} and η indicate the effective Lamé's constants and the elastic

loss factor, respectively. λ_{eff} is obtained through the equation $\kappa_{\text{eff}} = \lambda_{\text{eff}} + (2/3)\mu_{\text{eff}}$. As shown in Fig. 4, we obtain smooth curves in the whole frequency range regardless of the sign of the effective mass density. It is worth mentioning that the spring model is utilized only in the negative mass region, which proves in another way that the model is valid for acoustic metamaterials with negative parameters. Region A shown in Fig. 4 represents the positive effective mass frequency range below the resonant frequency, while region B represents the negative mass frequency range corresponding to the shadow area shown in Fig. 3. We can see from the figure that for $\eta = 0$, remarkable peaks appear in region A, which is due to the variation of the effective density of the locally resonant acoustic metamaterial coating caused by the first-order resonance. In contrast, no remarkable peaks are discovered in region B. For $\eta = 0.3$, we get a dramatic weakening of the scattering in region A, especially in the frequencies where the peaks appear for $\eta = 0$. In addition, a weakening of the scattering, through not dramatic, is also discovered in the negative parameter region B for $\eta = 0.3$, where the scattering is commonly supposed to be strengthened. However, in contrast to the case $\eta = 0$, the scattering enhances roughly at a frequency of $f = 525$ Hz, which is close to the first-order anti-resonant frequency of the coating.

To clarify the phenomena, an angular pattern of the scattering form function in the far field is plotted against the angle θ at the frequency $f = 525$ Hz, as shown in Fig. 5. We can see from the figure that the intensities of scattering from the coated shell for loss factors $\eta = 0$ and $\eta = 0.3$ are almost the same around the forward direction. However, in the other directions, the coated shell with loss factor $\eta = 0.3$ becomes a much stronger scatterer in contrast to the case $\eta = 0$. This may be caused by the enhancement of the stiffness of the coating when the viscosity is introduced.

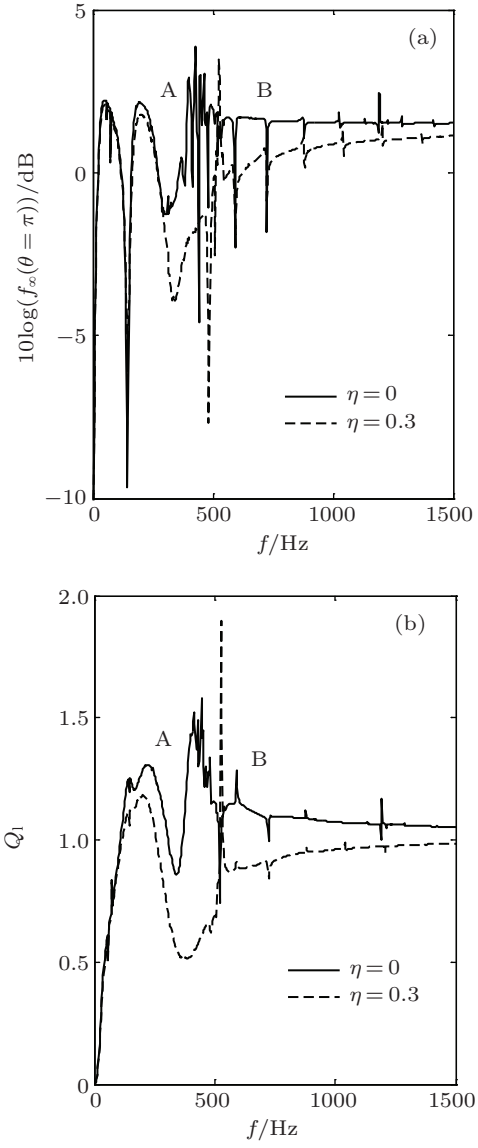


Fig. 4. (a) Calculated backscattering form function $f_\infty(\theta = \pi)$ versus frequency. (b) Calculated total scattering cross section Q_l versus frequency. The solid and dashed curves represent the cases of different elastic loss factors.

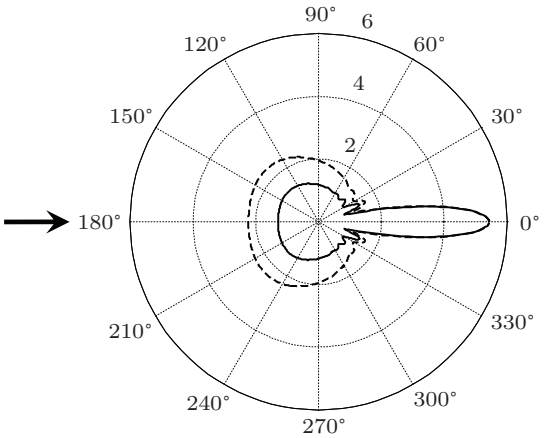


Fig. 5. Angular pattern of the far-field scattering form function plotted against θ at the frequency $f = 525$ Hz. The solid and dashed curves represent the cases of different elastic loss factors.

4. Conclusion

In summary, we have theoretically investigated the acoustic scattering of a submerged cylindrical shell coated with locally resonant acoustic metamaterials. It is shown that the spring model is valid to describe the elastic wave propagation in the thin metamaterial layer with negative mass. The viscosity leads to obvious scattering attenuations in both the positive and negative mass regions near the resonant frequency. Further studies are needed to discuss how the parameters of the locally resonant acoustic metamaterial coating affect the acoustic scattering of the cylindrical shell.

References

[1] Liu Z Y, Zhang X X, Mao Y W, Zhu Y Y, Yang Z Y, Chan C T and Sheng P 2000 *Science* **289** 1734
[2] Fok L, Ambati M and Zhang X 2008 *MRS Bullentin* **33** 931
[3] Fang N, Xi D J, Xu J Y, Ambati M, Srituravanich W, Sun C and Zhang X 2006 *Nature Mater.* **5** 452
[4] Cheng Y, Xu J Y and Liu X J 2008 *Phys. Rev.* B **77** 045134

[5] Cheng Y, Xu J Y and Liu X J 2008 *Appl. Phys. Lett.* **92** 051913
[6] Fok L and Zhang X 2011 *Phys. Rev.* B **83** 214304
[7] Ding C L, Zhao X P, Hao L M and Zhu W R 2011 *Acta Phys. Sin.* **60** 044301 (in Chinese)
[8] He Z J, Qiu C Y, Cheng L, Xiao M, Deng K and Liu Z Y 2010 *Europhys. Lett.* **91** 54004
[9] Naify C J, Chang C M, Mcknight G and Nutt S 2010 *J. Appl. Phys.* **108** 114905
[10] Ao X and Chan C T 2008 *Phys. Rev.* E **77** 025601
[11] Zhang S, Yin L L and Fang N 2009 *Phys. Rev. Lett.* **102** 194301
[12] Bobrovnitskiĭ Y I 2008 *Acoust. Phys.* **54** 879
[13] Zhou X M, Hu G K and Lu T J 2008 *Phys. Rev.* B **77** 024101
[14] Bobrovnitskiĭ Y I 2010 *New J. Phys.* **12** 043049
[15] Zhao H G, Liu Y Z, Wen J H, Yu D L, Wang G and Wen X S 2006 *Chin. Phys. Lett.* **23** 2132
[16] Zhao H G, Liu Y Z, Wen J H, Yu D L and Wen X S 2007 *Phys. Lett.* A **367** 224
[17] Zhao H G, Liu Y Z, Yu D L, Wang G, Wen J H and Wen X S 2007 *J. Sound Vib.* **303** 185
[18] Ni Q and Cheng J C 2007 *J. Appl. Phys.* **101** 073515
[19] Zhou X M and Hu G K 2009 *Phys. Rev.* B **79** 195109
[20] Mei J, Liu Z Y, Wen W J and Sheng P 2007 *Phys. Rev.* B **76** 134205
[21] Huang W, Wang Y J and Rokhlin S I 1996 *J. Acoust. Soc. Am.* **99** 2742
[22] Wang Y J and Zhu W Y 1996 *Chin. Phys. Lett.* **13** 20
[23] Xi D P 1998 *Bessel Functions* (Beijing: China Higher Education Press) p. 13
[24] Huang W, Rokhlin S I and Wang Y J 1997 *J. Acoust. Soc. Am.* **101** 2031